Adapted IMEX numerical methods for reaction-diffusion problems

Raffaele D'Ambrosio, Martina Moccaldi, Beatrice Paternoster

Abstract—The treatise is focused on the numerical solution of λ-ω reaction-diffusion problems, by means of a suitably adapted method of lines. Due to the non linearity of the vector field and the oscillatory behaviour of the solution, we propose to combine a spatial semidiscretization of the operator through trigonometrically fitted finite differences with an IMEX integration in time. Accuracy and stability properties of the overall numerical scheme are proved and experiments confirming the effectiveness of the approach are also provided.

Keywords—Reaction-diffusion problems periodic plane wave solutions trigonometrical fitting adapted method of lines IMEX methods.

I. Introduction

This paper is devoted to the numerical solution of reaction-diffusion systems of the following type

$$\begin{aligned} u_t &= u_{xx} + \lambda(r)u - \omega(r)v \\ v_t &= v_{xx} + \omega(r)u + \lambda(r)v \end{aligned} \tag{I.1}$$

with $u, v : [0,\infty) \times [0,T] \longrightarrow \mathbb{R}$, $r = \sqrt{u^2+v^2}$, $\omega(0) > 0$, $\lambda(0) > 0$.

These problems are frequently denoted as λ-ω problems, since their qualitative properties are governed by the form of the two functions $\lambda(r)$ and $\omega(r)$ appearing in (I.1) (see [62], [67] and references therein). An interesting qualitative feature that has made these problems widely used in applications [3], [56], [57], [66], [68], [69], [71]–[73], is given by the generation of travelling waves as fundamental solutions [62]. Such a feature is desirable for models in Life Science, since many cell cycles behave as driven by an autonomous biochemical oscillator [51]. In particular, λ-ω reaction-diffusion systems model problems having a limit cycle in reaction kinetics, such as in [3], which is proved to correspond to an isolated zero of $\lambda(r)$ [67].

As shown in [62], the exact solution of (I.1) admits the following parametric representation

$$\begin{aligned} u(x,t) &= \widehat{r}\cos(\omega(\widehat{r})t \pm \sqrt{\lambda(\widehat{r})}x), \\ v(x,t) &= \widehat{r}\sin(\omega(\widehat{r})t \pm \sqrt{\lambda(\widehat{r})}x), \end{aligned} \tag{I.2}$$

depending on the parameter $\widehat{r} \in \mathbb{R}$ such that $\lambda(\widehat{r}) > 0$. This expression, though useful to infer a qualitative behaviour of the solution, is actually not computable since it depends on the unknown parameter $\widehat{r}$. However, it is important to realize that it is a periodic plane wave, so it has constant shape and speed and oscillates both in space and in time and this information can be fruitfully used in order to assess an accurate and cheap numerical integrator.

Indeed, since the periodic behaviour of the solution is known, the natural idea is that of developing a numerical method that exploits this information as much as possible, following the lines drawn in [6], [15]–[17], [22], [28]–[31], [34], [35], [37], [39], [44]–[46], where *special purpose* numerical methods have been introduced by means of the so-called exponential fitting technique [61], [63]. Standard numerical methods could indeed strongly reduce the stepsize in order to reproduce the oscillatory behaviour along the numerical dynamics.

Classically, a *general purpose* formula is constructed in order to be exact (within round-off error) on polynomials up to a certain degree. However, when the exact solution of a problem has a particular a priori known character (e.g. periodicity, oscillations, exponential decay), classical methods could require a very small stepsize to accurately reproduce it, thus extremely increasing the computational burden. In this case, it may be convenient to use fitted formulae that are exact on functions other than polynomials: this idea gave rise to the birth of exponential fitting (see [61], [63] and references therein). The basis functions are chosen according to the information known a priori about the exact solution and belong to a finite-dimensional space called *fitting space*. Of course, the chosen basis functions also depend on a parameter connected to the solution, whose value is clearly unknown. As a consequence, non-polynomially fitted formulae have variable coefficients relying on this parameter instead of classical formulae that are characterized by constant coefficients.

In summary, an accurate and efficient numerical method based on exponential fitting has to rely on a suitable fitting space and on a cheap - but accurate - procedure for the estimate of the unknown parameters. Of course, these aspects can be well treated if a priori informations, given by theoretical studies on the problem, are known on the qualitative behaviour of the solution. For instance, as it regards the numerical solution of (I.1), the known parametrization (I.2) given in [62] not only suggests to choose a fitting space based on trigonometric functions, but also gives an idea of the spatial and temporal frequencies, whose knowledge can be exploited for a cheap computation of the unknown parameters, thus avoding expensive procedures based on solving nonlinear systems of equations as in [49], [50].

In this paper we extend the idea introduced in [39], where the problem (I.1) has been semi-discretized in space by the method of lines based on trigonometrically fitted finite differences. Then, the resulting system of ordinary differen-

Raffaele D'Ambrosio: Department of Engineering and Computer Science and Mathematics, University of L'Aquila, Italy, e-mail: raffaele.dambrosio@univaq.it

Martina Moccaldi and Beatrice Paternoster: Department of Mathematics, University of Salerno, Italy, e-mail: {mmoccaldi,beapat}@unisa.it

tial equations has been solved by standard time integrators, neglecting the form of the system. Here, we aim to suggest an overall numerical scheme taking into account the nature of the problem more closely. Indeed, the semi-discretized system has the form

$$y' = Ay + f(y)$$

where A is a matrix whose size depends on the number of points chosen for the spatial semi-discretization and $f(y)$ is a vector-valued function. Such a system clearly exhibits stiff components (arising from the diffusion term) and nonlinear ones (coming from the reaction term), dictated by the expressions of λ and ω which are usually chosen as [67]

$$\lambda(r) = \lambda_0 - r^p, \quad \omega(r) = \omega_0 - r^p, \tag{I.3}$$

with $p > 0$, $\lambda_0 > 0$ and $\omega_0 > 0$. Hence, since the problem has components of different nature, it is more natural to differently treat them, by means of implicit-explicit (IMEX) numerical methods that implicitly integrate the stiff terms and explicitly the other ones, following the classic idea [1], [2], [4], [5], [58].

In summary, the numerical scheme here proposed merges the adapted method of lines with an IMEX time solver, as described in Sections 2 and 3; Section 4 is devoted to present a rigorous analysis of accuracy and stability properties, while Section 5 presents some numerical experiments confirming the effectiveness of the approach, also in comparison with its classical counterpart based on general purpose methods; some conclusions are object of Section 6.

II. An adapted method of lines

We aim to solve problem (I.1) with λ and ω having the form (I.3) and equipped by the following initial conditions

$$u(x,0) = v(x,0) = A\exp(-\xi x), \tag{II.4}$$

and boundary conditions

$$\begin{aligned} u_x(0,t) = v_x(0,t) = 0,\\ \lim_{x\to+\infty} u(x,t) = \lim_{x\to+\infty} v(x,t) = 0. \end{aligned} \tag{II.5}$$

The dynamics occurs in an unbounded domain thus, for its numerical treatment, we consider as numerical domain its bounded counterpart

$$\overline{\mathcal{D}} := [0,X]\times[0,T] \tag{II.6}$$

where X is chosen large enough that any increase would only have negligible effects on the solution. Therefore, the considered numerical boundary conditions are given by

$$u_x(0,t) = v_x(0,t) = 0, \tag{II.7a}$$
$$u(X,t) = v(X,t) = 0. \tag{II.7b}$$

Following the method of lines (see [60], [64], [65] and references therein), we spatially discretize the domain (II.6)

$$\overline{\mathcal{D}}_h = \{(x_i,t) : x_i = ih, i = 0,\dots,N-1, h = X/(N-1)\},$$

where h is the spatial integration step. Then, we formulate equations (I.1) and conditions (II.4)-(II.7) in correspondence to each spatial grid point, obtaining the following system of ordinary differential equations [39]

$$\begin{aligned} {u'}_0(t) &= {u'}_2(t),\\ {v'}_0(t) &= {v'}_2(t),\\ {u'}_i(t) &= \Delta_n[u_i(t),h] + \lambda(r)u_i(t) - \omega(r)v_i(t),\\ {v'}_i(t) &= \Delta_n[v_i(t),h] + \omega(r)u_i(t) + \lambda(r)v_i(t),\\ {u'}_{N-1}(t) &= 0,\\ {v'}_{N-1}(t) &= 0, \end{aligned} \tag{II.8}$$

with $1 \le i \le N-2$, where

$$u_i(t) := u(x_i,t),\ v_i(t) = v(x_i,t), \quad 0 \le i \le N-1$$

and $\Delta_n[\Phi_i(t),h]$ (with $\Phi_i(t) = u_i(t)$ or $\Phi_i(t) = v_i(t)$) is the n-point fitted finite difference formula used to approximate the second spatial derivatives. The system is also combined with the initial conditions

$$u_i(0) = v_i(0) = A\exp(-\xi x_i), \quad 0 \le i \le N-1. \tag{II.9}$$

As in [39], [44], we approximate the second spatial derivatives of functions u and v by the three-point finite difference formula

$$\Delta_n[\Phi_i(t),h] = \frac{1}{h^2}\left(a_0\Phi_{i+1}(t) + a_1\Phi_i(t) + a_2\Phi_{i-1}(t)\right) \tag{II.10}$$

and, taking into account the known parametrization of the wavefront (I.2), we employ the adapted version of (II.10) based on the trigonometrical fitting space

$$\mathcal{F} = \{1, \sin(\mu x), \cos(\mu x)\}, \tag{II.11}$$

with spatial frequency $\mu \in \mathbb{R}$. Thus, as given in [44], the expressions of the coefficients a_0, a_1 and a_2 are determined by imposing the exactness of (II.10) on the space (II.11), obtaining

$$\begin{aligned} a_0(z) &= \frac{z^2}{2(1-\cos z)} = a_2(z),\\ a_1(z) &= -\frac{z^2}{(1-\cos z)}, \end{aligned} \tag{II.12}$$

with $z = \mu h$. Of course, it is evident that such coefficients are no longer constant, as in the classical polynomial case, but are functions of z. In general, $z \neq 0$ because $h \neq 0$ and the frequency is not null in the case of periodic solutions. Nevertheless, when z tends to 0, the variable coefficients (II.12) tend to the classical ones:

$$a_0 = a_2 = 1, \quad a_1 = -2. \tag{II.13}$$

Hence, the trigonometrically fitted formula retains the same order of accuracy of the corresponding classical one as shown in [44], which is equal to 2.

As aforementioned, the actual employ of trigonometrically fitted formulae relies on the accurate computation of μ, on which the coefficients (II.12) depend on. The knowledge of the parametrization (I.2) can give an approximation strategy based on the natural choice [39] of the same spatial frequency

$$\mu_{ij} = \sqrt{|\lambda(r_{ij})|} \tag{II.14}$$

where

$$r_{ij} = \sqrt{u_{ij}^2 + v_{ij}^2} \tag{II.15}$$

with $u_{ij} \approx u(x_i, t_j)$, $v_{ij} \approx v(x_i, t_j)$. It is important to highlight that, even if the spatial frequency of the wavefront (I.2) is constant, it is convenient to update its approximation at each grid point for accuracy purposes [59], [61]. Thus, the proposed estimate is suggested by the problem and does not increase the computational cost because it does not require optimization techniques or the resolution of nonlinear systems of equations as in [49], [59] and references therein.

III. IMEX time integration

IMEX methods are widely used when a problem has components of different nature, requiring different computational efforts (see [1], [2], [4], [5], [58] and references therein). Indeed, a totally explicit method can require strong restrictions on the stepsize to guarantee the stability, especially if it integrates stiff terms. Stiff problems are better integrated by implicit methods, however these methods are more expensive and more complex than explicit ones. IMEX methods implicitly integrate only the components that need it (stiff components) and explicitly integrate the other ones.

Differently from [39], we aim to propose an IMEX time integration of the semi-discretized system of ordinary differential equations (II.8), due to its intrinsic nature. Indeed, that system can be regarded in a more compact form as

$$\begin{aligned} U'(t) &= A(z)U(t) + \Lambda(r)U(t) - \Omega(r)V(t) \\ V'(t) &= A(z)V(t) + \Omega(r)U(t) + \Lambda(r)V(t) \end{aligned} \tag{III.16}$$

with

$$U(t) = \begin{bmatrix} u_1(t) \\ u_2(t) \\ \vdots \\ u_{N-2}(t) \end{bmatrix},$$

$$V(t) = \begin{bmatrix} v_1(t) \\ v_2(t) \\ \vdots \\ v_{N-2}(t) \end{bmatrix},$$

$$A(z) = \frac{\gamma(z)}{h^2} \begin{bmatrix} -2 & 2 & & & \\ 1 & -2 & 1 & & \\ & \ddots & \ddots & & \\ & & 1 & -2 \end{bmatrix},$$

$$\gamma(z) = \frac{z^2}{2(1-\cos z)},$$

$$\Lambda(r) = \begin{bmatrix} \lambda(r) & & & \\ & \lambda(r) & & \\ & & \ddots & \\ & & & \lambda(r) \end{bmatrix},$$

$$\Omega(r) = \begin{bmatrix} \omega(r) & & & \\ & \omega(r) & & \\ & & \ddots & \\ & & & \omega(r) \end{bmatrix}.$$

For the time discretization, we select M equidistant points

$$t_j = jk, \quad j = 1, 2, \ldots, M$$

in $[0, T]$, where k is the chosen uniform time step, and apply the linear first order IMEX Euler method [1]

$$\Phi^{j+1} = \Phi^j + kg(\Phi^{j+1}) + kf(\Phi^j)$$

where g is the diffusion term and f is the reaction term. Thus, the implicit part of the integrator only involves the stiff components of the solution. Hence, the numerical scheme for (III.16) assumes the form

$$\begin{aligned} U^{j+1} &= U^j + kA^{j+1}U^{j+1} + k\Lambda^j U^j - k\Omega^j V^j \\ V^{j+1} &= V^j + kA^{j+1}V^{j+1} + k\Omega^j U^j + k\Lambda^j V^j \end{aligned} \tag{III.17}$$

or, in a more compact form,

$$W^{j+1} = W^j + k\mathcal{A}^{j+1}W^{j+1} + k\Gamma^j W^j \tag{III.18}$$

where

$$W = \begin{bmatrix} U \\ V \end{bmatrix},$$

$$\mathcal{A}^{j+1} = \begin{bmatrix} A^{j+1} & \\ & A^{j+1} \end{bmatrix}, \quad \Gamma^j = \begin{bmatrix} \Lambda^j & -\Omega^j \\ \Omega^j & \Lambda^j \end{bmatrix}.$$

We observe that the matrices Γ and $\mathcal{A}$ depend on r that is approximated by (II.15), so they have to be recomputed at each time step.

IV. Accuracy and stability analysis

We now aim to analyze accuracy and stability properties of the novel numerical scheme (III.18), which originates from exponentially fitted spatial semi-discretization and IMEX time integration. The overall scheme will be denoted as IMEX-EF in the remainder of the treatise.

A. Convergence analysis

First of all, let us prove the consistency of the IMEX-EF scheme (III.18) with the problem (I.1). As it will be clear during the proof, the order of consistency of the numerical scheme will also be computed: as expected, since the finite difference employed in spatial semidiscretization has order 2 and the IMEX-Euler method has order 1, we are going to prove that the order of consistency is $\mathcal{O}(z^2) + \mathcal{O}(k)$, where $z = \mu h$ as in (II.12) and k is the time stepsize.

Theorem IV.1. *The IMEX-EF method* (III.18) *is consistent with the problem* (I.1) *with initial conditions* (II.4) *and boundary conditions* (II.7) *and the order of consistency is* $\mathcal{O}(z^2) + \mathcal{O}(k)$.

Proof: We report here the proof for the u component only, since that for the v component of the solution is obtained in the same way. We define the local truncation error of the method as the residual operator

$$\begin{aligned} P_{h,k}[u] = \frac{u(x_i, t_{j+1}) - u(x_i, t_j)}{k} - F_1\left(u(x_i, t_j), v(x_i, t_j)\right) \\ - \frac{\gamma(z)}{h^2}\left(u(x_{i+1}, t_{j+1}) - 2u(x_i, t_{j+1}) + u(x_{i-1}, t_{j+1})\right), \end{aligned} \tag{IV.19}$$

where $F_1(u(x_i,t_j),v(x_i,t_j)) = \lambda(r)u(x_i,t_j) - \omega(r)v(x_i,t_j)$. We next compute the following Taylor series expansions useful to suitably rewrite the residual operator (IV.19)

$$u(x_i,t_{j+1}) = u(x_i,t_j) + ku_t^{i,j} + \frac{k^2}{2}u_{tt}^{i,j} + \mathcal{O}(k^3), \tag{IV.20a}$$

$$u(x_{i+1},t_{j+1}) = u(x_i,t_{j+1}) + hu_x^{i,j+1} + \frac{h^2}{2}u_{xx}^{i,j+1} + \mathcal{O}(h^3), \tag{IV.20b}$$

$$u(x_{i-1},t_{j+1}) = u(x_i,t_{j+1}) - hu_x^{i,j+1} + \frac{h^2}{2}u_{xx}^{i,j+1} + \mathcal{O}(h^3), \tag{IV.20c}$$

$$u_{xx}^{i,j+1} = u_{xx}^{i,j} + ku_{txx}^{i,j} + \frac{k^2}{2}u_{ttxx}^{i,j} + \mathcal{O}(k^3), \tag{IV.20d}$$

where

$$u_t^{i,j} = \left(\frac{\partial u}{\partial t}\right)_{i,j},\ u_{tt}^{i,j} = \left(\frac{\partial^2 u}{\partial t^2}\right)_{i,j},$$

$$u_x^{i,j+1} = \left(\frac{\partial u}{\partial x}\right)_{i,j+1},\ u_{xx}^{i,j+1} = \left(\frac{\partial^2 u}{\partial x^2}\right)_{i,j+1},$$

$$u_{xx}^{i,j} = \left(\frac{\partial^2 u}{\partial x^2}\right)_{i,j},\quad u_{txx}^{i,j} = \left(\frac{\partial^3 u}{\partial t x^2}\right)_{i,j},$$

$$u_{ttxx}^{i,j} = \left(\frac{\partial^2 4u}{\partial t^2 x^2}\right)_{i,j}.$$

Equation (IV.20a) leads to

$$\frac{u(x_i,t_{j+1}) - u(x_i,t_j)}{k} = u_t^{i,j} + \frac{k}{2}u_{tt}^{i,j} + \mathcal{O}(k^2),$$

while the sum between (IV.20b) and (IV.20c), taking into account (IV.20d), gives

$$\begin{aligned} u(x_{i+1},t_{j+1}) - 2u(x_i,t_{j+1}) + u(x_{i-1},t_{j+1}) \\ = h^2u_{xx}^{i,j} + h^2ku_{txx}^{i,j} + \mathcal{O}(k^2h^2). \end{aligned}$$

We now expand $\gamma(z)$ in power series, obtaining

$$\gamma(z) = 1 + \frac{z^2}{12} + \frac{z^4}{240} + \mathcal{O}(z^6).$$

Hence, the local truncation error (IV.19) assumes the form

$$\begin{aligned} P_{h,k}[u] &= u_t^{i,j} + \frac{k}{2}u_{tt}^{i,j} + \mathcal{O}(k^2) - F_1(u(x_i,t_j),v(x_i,t_j)) \\ &\quad - \frac{1}{h^2}\left(1 + \frac{z^2}{12} + \frac{z^4}{240} + \mathcal{O}(z^6)\right) \\ &\quad \cdot \left(h^2u_{xx}^{i,j} + h^2ku_{txx}^{i,j} + \mathcal{O}(h^2k^2)\right) \\ &= u_t^{i,j} - F_1(u(x_i,t_j),v(x_i,t_j)) \\ &\quad - u_{xx}^{i,j} + k\left(\frac{1}{2}u_{tt}^{i,j} - u_{txx}^{i,j}\right) + \mathcal{O}(k^2) \\ &\quad - \left(\frac{z^2}{12} + \frac{z^4}{240} + \mathcal{O}(z^6)\right) \\ &\quad \cdot \left(u_{xx}^{i,j} + ku_{txx}^{i,j} + \mathcal{O}(k^2)\right). \end{aligned}$$

Since $u(x,t)$ and $v(x,t)$ are the components of the exact solution of the problem (I.1), they fulfill the equation

$$u_t^{i,j} - u_{xx}^{i,j} - F_1(u(x_i,t_j),v(x_i,t_j)) = 0.$$

Therefore, the local truncation error becomes

$$\begin{aligned} P_{h,k}[u] &= k\left(\frac{1}{2}u_{tt}^{i,j} - u_{txx}^{i,j}\right) + \mathcal{O}(k^2) - \frac{z^2}{12}u_{xx}^{i,j} \\ &\quad - \left(\frac{z^2}{12} + \frac{z^4}{240} + \mathcal{O}(z^6)\right)\left(ku_{txx}^{i,j} + \mathcal{O}(k^2)\right) \\ &\quad - \left(\frac{z^4}{240} + \mathcal{O}(z^6)\right)u_{xx}^{i,j} \\ &= \mathcal{O}(k) + \mathcal{O}(z^2). \end{aligned}$$

■

We now focus our attention to convergence analysis, by rigorously proving the overall boundedness of the global error.

Theorem IV.2. *Suppose that the vector valued function $F(W(\cdot,t_j)) = \Gamma W(\cdot,t_j)$ is smooth enough and satisfies the bound*

$$\|\nabla F\|_\infty \le F_{max}.$$

Then, the global error

$$E^{j+1} = W(\cdot,t_{j+1}) - W^{j+1}$$

fulfills the bound

$$\begin{aligned} \left\|E^{j+1}\right\|_\infty &\le (1+kF_{max})^j \\ &\quad \cdot \sum_{\beta=0}^{j} \frac{1}{(1-kA_{max})^{\beta+1}} \max_{s=1,2,\ldots,j+1} \left\|\mathcal{R}_{h,k}^{(s)}\right\|_\infty, \end{aligned}$$

being A_{max} an upper bound for $\|\mathcal{A}\|_\infty$ and $\mathcal{R}_{h,k}^{(j+1)} = \mathcal{O}(k) + \mathcal{O}(z^2)$. In other terms, under the above hypothesis, the IMEX-EF method (III.18) *is convergent.*

Proof: The discretization error in a fixed time grid point t_{j+1} is given by

$$E^{j+1} = W(\cdot,t_{j+1}) - W^{j+1},$$

where $W(\cdot,t_{j+1})$ is the exact solution in t_{j+1}. Consistency of the method implies that

$$W(\cdot,t_{j+1}) = W(\cdot,t_j) + k\,\mathcal{A}\,W(\cdot,t_{j+1}) + kF(W(\cdot,t_j)) + \mathcal{R}_{h,k}^{(j+1)},$$

where $\mathcal{R}_{h,k}^{(j+1)} = \mathcal{O}(k) + \mathcal{O}(z^2)$ and $F(W(\cdot,t_j)) = \Gamma W(\cdot,t_j)$. Therefore, the discretization error assumes the form

$$\begin{aligned} E^{j+1} &= W(\cdot,t_j) + k\,\mathcal{A}\,W(\cdot,t_{j+1}) + kF(W(\cdot,t_j)) \\ &\quad + \mathcal{R}_{h,k}^{(j+1)} - W^j - k\,\mathcal{A}\,W^{j+1} - kF(W^j) \\ &= E^j + k\,\mathcal{A}\,E^{j+1} + k[F(W(\cdot,t_j)) - F(W^j)] + \mathcal{R}_{h,k}^{(j+1)}. \end{aligned}$$

The regularity assumption on F allows us to apply the Mean Value Theorem, leading to

$$\begin{aligned} \left\|F(W(\cdot,t_j)) - F(W^j)\right\|_\infty &= \|\nabla F\|_\infty \left\|W(\cdot,t_j) - W^j\right\|_\infty \\ &= \|\nabla F\|_\infty \left\|E^j\right\|_\infty. \end{aligned}$$

Moreover, since F has bounded derivative and satisfies $\|\nabla F\|_\infty \leq F_{max}$, we have

$$\left\|F(W(\cdot,t_j)) - F(W^j)\right\|_\infty \leq F_{max}\left\|E^j\right\|_\infty.$$

We next consider the following bound

$$\|\mathcal{A}\|_\infty = \|A\|_\infty = \frac{4\gamma}{h^2} = \frac{2\mu^2}{1-\cos(z)} \leq A_{max}$$

due to the fact that the values μ and h are bounded themselves because they are the spatial frequency and the spatial stepsize, respectively. Then, the norm of the discretization error is given by

$$\begin{aligned}\left\|E^{j+1}\right\|_\infty &\leq \left\|E^j\right\| + k\|\mathcal{A}\|_\infty \left\|E^{j+1}\right\|_\infty \\ &\quad + k\left\|F(W(\cdot,t_j)) - F(W^j)\right\|_\infty + \left\|\mathcal{R}_{h,k}^{(j+1)}\right\|_\infty \\ &\leq \left\|E^j\right\| + kA_{max}\left\|E^{j+1}\right\|_\infty \\ &\quad + kF_{max}\left\|E^j\right\|_\infty + \left\|\mathcal{R}_{h,k}^{(j+1)}\right\|_\infty.\end{aligned}$$

The last inequality can be rewritten by isolating the discretization error at $j+1$ step

$$\left\|E^{j+1}\right\|_\infty \leq \frac{1+kF_{max}}{1-kA_{max}}\left\|E^j\right\|_\infty + \frac{1}{1-kA_{max}}\left\|\mathcal{R}_{h,k}^{(j+1)}\right\|_\infty. \tag{IV.21}$$

We denote

$$Q = \frac{1+kF_{max}}{1-kA_{max}} \quad \text{and} \quad S = \frac{1}{1-kA_{max}}$$

and recursively apply Equation (IV.21) until the discretization error at first step appears, as follows:

$$\begin{aligned}\left\|E^{j+1}\right\|_\infty &\leq Q\left\|E^j\right\|_\infty + S\left\|\mathcal{R}_{h,k}^{(j+1)}\right\|_\infty \\ &\leq Q\left[Q\left\|E^{j-1}\right\|_\infty + S\left\|\mathcal{R}_{h,k}^{(j)}\right\|_\infty\right] + S\left\|\mathcal{R}_{h,k}^{(j+1)}\right\|_\infty \\ &\leq Q^2\left\|E^{j-1}\right\|_\infty + QS\left\|\mathcal{R}_{h,k}^{(j)}\right\|_\infty + S\left\|\mathcal{R}_{h,k}^{(j+1)}\right\|_\infty \\ &\leq Q^3\left\|E^{j-2}\right\|_\infty + Q^2S\left\|\mathcal{R}_{h,k}^{(j-1)}\right\|_\infty \\ &\quad + QS\left\|\mathcal{R}_{h,k}^{(j)}\right\|_\infty + S\left\|\mathcal{R}_{h,k}^{(j+1)}\right\|_\infty \\ &\vdots \\ &\leq Q^{j+1}\left\|E^0\right\|_\infty + Q^jS\left\|\mathcal{R}_{h,k}^{(1)}\right\|_\infty + \cdots \\ &\quad + QS\left\|\mathcal{R}_{h,k}^{(j)}\right\|_\infty + S\left\|\mathcal{R}_{h,k}^{(j+1)}\right\|_\infty.\end{aligned}$$

Of course $\left\|E^0\right\|_\infty = 0$. Thus, for each j we obtain

$$\begin{aligned}\left\|E^{j+1}\right\|_\infty &\leq S[Q^j + Q^{j-1} + \cdots + Q + 1]\max_{s=1,2,\ldots,j+1}\left\|\mathcal{R}_{h,k}^{(s)}\right\|_\infty \\ &\leq (1+kF_{max})^j \\ &\quad \cdot \sum_{\beta=0}^{j}\frac{1}{(1-kA_{max})^{\beta+1}}\max_{s=1,2,\ldots,j+1}\left\|\mathcal{R}_{h,k}^{(s)}\right\|_\infty,\end{aligned}$$

tending to 0 as h and k tend to 0. ∎

We observe that the proofs of above Theorems IV.1 and IV.2 do not depend on the choice of the parameter μ and the expression of the functions λ and ω appearing in (I.1).

B. Stability analysis

The following theorem provides a simple criterion for the analysis of stability properties of the IMEX-EF method. The proof is completely independent on the way the parameter μ is estimated.

Theorem IV.3. *The method* (III.18) *is stable if*

$$\left\|(\mathbb{I} - k\mathcal{A})^{-1}\right\| \leq 1.$$

Proof: Following the idea in [70], we aim to prove stability by controlling the propagation of the error caused by an incoming perturbation. To do this, we perturb the solution W^j as follows

$$\widetilde{W}^j = W^j + \delta.$$

Since

$$\begin{aligned}W^{j+1} &= (\mathbb{I} - k\mathcal{A})^{-1}(W^j + k\Gamma^j W^j), \\ \widetilde{W}^{j+1} &= (\mathbb{I} - k\mathcal{A})^{-1}(\widetilde{W}^j + k\widetilde{\Gamma}^j\widetilde{W}^j),\end{aligned}$$

the error due to the perturbation is given by

$$E^{j+1} = W^{j+1} - \widetilde{W}^{j+1} = (\mathbb{I} - k\mathcal{A})^{-1}[E^j + k(\Gamma^j W^j - \widetilde{\Gamma}^j\widetilde{W}^j)]$$

and its norm is bounded by

$$\begin{aligned}\left\|E^{j+1}\right\|_\infty &\leq \left\|(\mathbb{I} - k\mathcal{A})^{-1}\right\|_\infty \\ &\quad \cdot \left(\left\|E^j\right\|_\infty + k\left\| \Gamma^j W^j - \widetilde{\Gamma}^j\widetilde{W}^j \right\|_\infty \right) \\ &\leq \left\|(\mathbb{I} - k\mathcal{A})^{-1}\right\|_\infty \\ &\quad \cdot \left(\left\|E^j\right\|_\infty - k\left(\| \Gamma^j W^j \|_\infty - \left\| \widetilde{\Gamma}^j\widetilde{W}^j \right\|_\infty \right) \right).\end{aligned} \tag{IV.22}$$

We now bound the nonlinear terms in (I.3) by

$$\begin{aligned}|\lambda(r_{i,j})| &= |\lambda_0 - r_{i,j}^p| \leq \lambda_0 + r_{i,j}^p, \\ |\omega(r_{i,j})| &= |\omega_0 - r_{i,j}^p| \leq \omega_0 + r_{i,j}^p.\end{aligned}$$

Since

$$r_{i,j}^p = (u_{i,j}^2 + v_{i,j}^2)^{p/2} \leq (u_{i,j} + v_{i,j})^p$$

we obtain

$$\begin{aligned}\left\|\Gamma^j\right\|_\infty &:= \max_{i=1,\ldots,2(N-2)}\{|\lambda(r_{i,j})| + |\omega(r_{i,j})|\} \\ &\leq \theta_0 + 2\max_{i=1,\ldots,2(N-2)}\left\{r_{i,j}^p\right\} \\ &\leq \theta_0 + 2\max_{i=1,\ldots,2(N-2)}\{(u_{i,j} + v_{i,j})^p\} \\ &\leq \theta_0 + 2^{p+1}\left\|W^j\right\|_\infty^p,\end{aligned}$$

where $\theta_0 = \lambda_0 + \omega_0$. Thus, we have

$$\begin{aligned}\| \Gamma^j W^j \|_\infty - \left\|\widetilde{\Gamma}^j\widetilde{W}^j\right\|_\infty &\leq \| \Gamma^j \|_\infty \|W^j\|_\infty + \left\|\widetilde{\Gamma}^j\right\|_\infty \left\|\widetilde{W}^j\right\|_\infty \\ &\leq \left[\theta_0 + 2^{p+1}\left\|W^j\right\|_\infty^p\right]\|W^j\|_\infty \\ &\quad + \left[\theta_0 + 2^{p+1}\left\|\widetilde{W}^j\right\|_\infty^p\right]\left\|\widetilde{W}^j\right\|_\infty \\ &\leq \theta_0\left[\|W^j\|_\infty + \left\|\widetilde{W}^j\right\|_\infty\right] \\ &\quad + 2^{p+1}\left[\|W^j\|_\infty^{p+1} + \left\|\widetilde{W}^j\right\|_\infty^{p+1}\right] \\ &\leq 3\theta_0 + 2\cdot 3^{p+1},\end{aligned}$$

where we use that $\left\|W^j\right\|_\infty \leq \widehat{r}$ and $\widehat{r} \leq \frac{3}{2}$. This last inequality is suggested by the results in [39], where the authors have shown that the numerical solution oscillates in $[-1.19, 1.19]$. Therefore, the norm of the error (IV.22) is

$$\begin{aligned}\left\|E^{j+1}\right\|_\infty &\leq \left\|(\mathbb{I}-k\mathcal{A})^{-1}\right\|_\infty \left(\left\|E^j\right\|_\infty - k(\theta_0 + 2\cdot 3^{p+1}) \right) \\ &\leq \left\|(\mathbb{I}-k\mathcal{A})^{-1}\right\|_\infty \left\|E^j\right\|_\infty .\end{aligned}$$

Last inequality immediately suggests the stability condition

$$\left\|(\mathbb{I}-k\mathcal{A})^{-1}\right\|_\infty \leq 1.$$

■

V. Numerical experiments

We now present some numerical results obtained by solving the system of PDEs (I.1) with the following values for the parameters as in [67]

$$\lambda_0 = 1, \quad \omega_0 = 2, \quad p = 1.8, \quad A = 0.1, \quad \xi = 0.8.$$

Fig.1 shows the numerical solution obtained by the new method IMEX-EF (III.18) based on the combination between the IMEX strategy and exponential fitting technique. We have chosen the rectangular domain $(x,t) \in [0,150] \times [0,60]$. It is useful to note that the spatial interval is large enough in order to justify the use of boundary conditions (II.7) instead of (II.5). The profile of the numerical solution is coherent with the theoretical expectations presented in [67]: indeed, the solution starts with an exponential decay and then evolves to a wavefront that moves through the domain with constant speed and shape. Moreover, this wave front is followed by periodic plane waves and the solution respects the boundary conditions.

We now compare the numerical results of the new method (III.18) with the analogous IMEX method combined with classical finite difference (II.10) depending on constant coefficients (II.13). As it is clear in Fig. 2 and Fig. 3 and in Table I, if the stepsize is increased, the numerical solution produced by the exponential fitting method is stable while that obtained by the classical approach results unstable. If the stepsize is reduced (so, when the numerical solution exhibits stable modes), we observe that the proposed IMEX-EF is somehow comparable with its classical counterpart. However, this benefits in accuracy could be largely improved by estimating better the parameter correlated to exponential fitting. The selection of this parameter is indeed a crucial issue in the exponential fitting procedure and can increase extremely the computational burden if it is carried out by solving nonlinear systems as, for instance, in [50]. The proposal to adopt an estimate of the parameter suggested by the problem does not increase the computational cost at all, but the accuracy is more compromised. In summary, the exponentially fitted version IMEX-EF is a more stabilized version of the IMEX-CLASS scheme, even when the value of the parameter is not accurately computed.

	h	k	error
IMEX-EF	3	1.5	$8 \cdot 10^{-1}$
IMEX-CLASS	3	1.5	2267848.05
IMEX-EF	3	0.5	$9.2 \cdot 10^{-3}$
IMEX-CLASS	3	0.5	$2.08 \cdot 10^{-2}$

TABLE I
COMPARISON BETWEEN THE IMEX-EF METHOD (III.18) AND THE SAME IMEX METHOD WITH STANDARD FINITE DIFFERENCE FORMULAE IN TERMS OF THE ERROR ON EXTREMITIES WHEN THEY ARE APPLIED TO THE PROBLEM (I.1) WITH INITIAL CONDITIONS (II.4), BOUNDARY CONDITIONS (II.7).

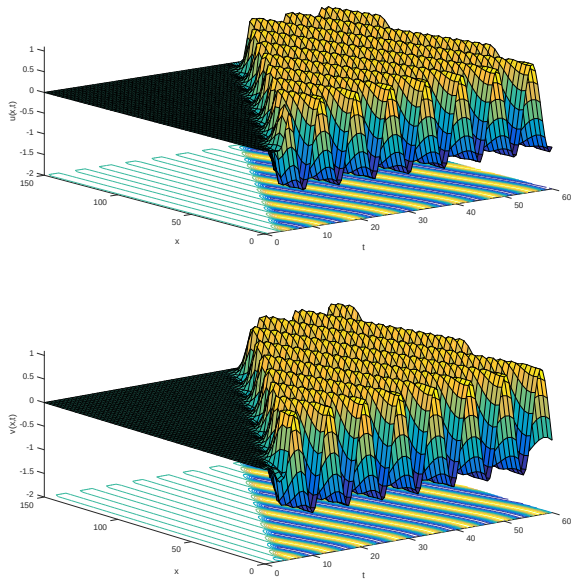

Fig. 1. Numerical solution of $\lambda - \omega$ reaction-diffusion system (I.1), with initial conditions (II.4) and boundary conditions (II.7) computed by the new method (III.18) with spatial stepsize $h = 3$ and time stepsize $k = 0.5$. The component $u(x,t)$ is depicted on the top and the component $v(x,t)$ is represented on the bottom.

VI. Conclusions

For the numerical solution of a reaction-diffusion problem of λ-ω type (I.1), we have introduced a novel numerical scheme which relies on qualitative behaviour of the solution, i.e. the wavefront described by (I.2), and the structure of the system of ordinary differential equations obtained by spatial semi-discretization through adapted finite differences. The overall numerical scheme is trigonometrically fitted in space and IMEX in time. The properties of the overall scheme are analyzed, with special emphasis to convergence and stability analysis, by also proving that it enables to improve the stability properties with respect to its classical counterpart, based on polynomials. Numerical experiments confirm that the IMEX-EF scheme is more stable than its classical counterpart, even when the unknown parameters on which the adapted schemes depend are not accurately estimated. This work is a preliminary study about the combination of trigonometrically fitted finite difference formulae and IMEX methods in the 1D case. As a future research, we aim to extend the presented ideas to 2D and 3D cases, where the construction of trigonometrically fitted finite difference formulae may be made

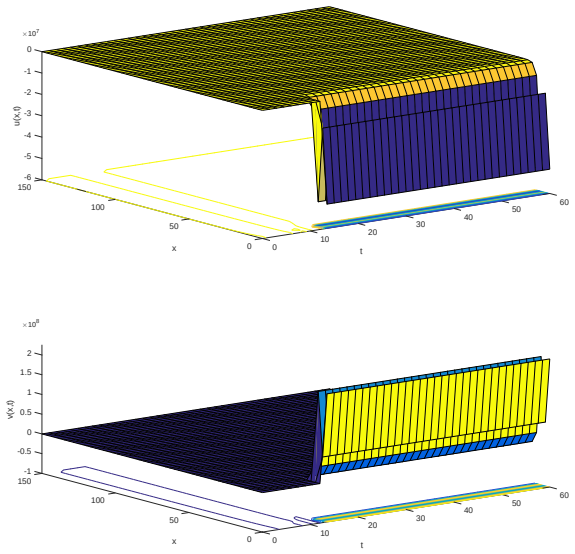

Fig. 2. Numerical solution of $\lambda - \omega$ reaction-diffusion system (I.1), with initial conditions (II.4) and boundary conditions (II.7) computed by a standard IMEX method with spatial stepsize $h = 3$ and time stepsize $k = 1.5$. The component $u(x,t)$ is depicted on the top and the component $v(x,t)$ is represented on the bottom.

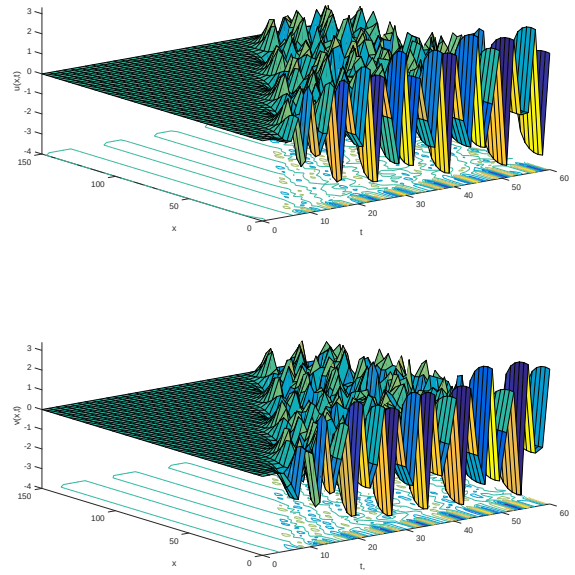

Fig. 3. Numerical solution of $\lambda - \omega$ reaction-diffusion system (I.1), with initial conditions (II.4) and boundary conditions (II.7) computed by the new method (III.18) with spatial stepsize $h = 3$ and time stepsize $k = 1.5$. The component $u(x,t)$ is depicted on the top and the component $v(x,t)$ is represented on the bottom.

more challenging by the presence of a different frequency in each spatial direction. Further issues will also regard the improvement to the accuracy of the adapted scheme in the stable modes, with respect to the classical IMEX scheme, also by means of adapted general time discretizations [24], [38], [40], [42]. The research will also be oriented to the application of analog techniques to stochastic problems [12], [13], [23], [36], problems with memory [8]–[11], [14], [18]–[21], [26], [32], [33], also in a structure-preserving or meshfree perspective [7], [25], [27], [43], [47], [48], [52]–[55].

ACKNOWLEDGMENT

The authors are members of GNCS-INDAM. This work is supported by GNCS-INDAM.

REFERENCES

[1] U.M. Ascher, S.J. Ruuth, B.T.R. Wetton, Implicit-Explicit methods for time-dependent partial differential equations, SIAM J. Numer. Anal. 32, 797–823 (1995).
[2] U.M. Ascher, S.J. Ruuth, R.J. Spiteri, Implicit-Explicit Runge-Kutta Methods for Time-Dependent Partial Differential Equations, Appl. Numer. Math. 25(2-3), 151–167 (1997).
[3] A. Atri, J. Amudson, D. Clapham, J. Sneyd, A single-pool model for intracellular calcium oscillations and waves in Xenopus laevis Oocyte, Biophysical Journal 65, 1727-1739 (1993).
[4] S. Boscarino, On an accurate third order implicit-explicit Runge-Kutta method for stiff problems, Appl. Numer. Math. 59(7), 1515–1528 (2009).
[5] S. Boscarino, Error analysis of IMEX Runge-Kutta methods derived from differential-algebraic systems, SIAM J. Numer. Anal. 45(4), 1600–1621 (2007).
[6] K. Burrage, A. Cardone, R. D'Ambrosio, B. Paternoster, Numerical solution of time fractional diffusion systems, Appl. Numer. Math. 116, 82–94 (2017).
[7] J. Butcher, R. D'Ambrosio, Partitioned general linear methods for separable Hamiltonian problems, Appl. Numer. Math. 117, 69–86 (2017).
[8] G. Capobianco, D. Conte, I. Del Prete, High performance numerical methods for Volterra equations with weakly singular kernels, J. Comput. Appl. Math., 228 (2009).
[9] G. Capobianco, D. Conte, An efficient and fast parallel method for Volterra integral equations of Abel type, J. Comput. Appl. Math., Vol 189/1-2 481-493 (2006).
[10] A. Cardone, D. Conte, Multistep collocation methods for Volterra Integro-Differential Equations, Appl. Math. Comput., 221, 770–785 (2013).
[11] A. Cardone, D. Conte, B. Paternoster, Two-step collocation methods for fractional differential equations, Discr. Cont. Dyn. Sys. B 23(7), 2709-2725 (2018).
[12] A. Cardone, R. D'Ambrosio, B. Paternoster, A spectral method for stochastic fractional differential equations, Appl. Numer. Math. 139, 115–119 (2019).
[13] A. Cardone, D. Conte, R. D'Ambrosio, B. Paternoster, Stability Issues for Selected Stochastic Evolutionary Problems: A Review, Axioms, doi: 10.3390/axioms7040091 (2018).
[14] A. Cardone, D. Conte, R. D'Ambrosio, B. Paternoster, Collocation Methods for Volterra Integral and Integro-Differential Equations: A Review, Axioms 7(3), 45 (2018).
[15] A. Cardone, R. D'Ambrosio, B. Paternoster, Exponentially fitted IMEX methods for advection-diffusion problems, J. Comput. Appl. Math. 316, 100–108 (2017).
[16] A. Cardone, R. D'Ambrosio, B. Paternoster, High order exponentially fitted methods for Volterra integral equations with periodic solution, Appl. Numer. Math. 114C,18–29 (2017).
[17] A. Cardone, D. Conte, R. D'Ambrosio, B.Paternoster, On the numerical treatment of selected oscillatory evolutionary problems, AIP Conf. Proc., 1863, 160004 (2017).
[18] A. Cardone, D. Conte, B. Paternoster, A family of Multistep Collocation Methods for Volterra Integro-Differential Equations, AIP Conf. Proc. 1168 (1), 2009.
[19] D. Conte, G. Califano, Optimal Schwarz Waveform Relaxation for fractional diffusion-wave equations, Appl. Numer. Math. 127, 125-141 (2018).
[20] D. Conte, G. Califano, Domain Decomposition Methods for a Class of Integro-Partial Differential Equations, AIP Conf. Proc. 1776, 090050 (2016).
[21] D. Conte, G. Capobianco, B. Paternoster, Construction and implementation of two-step continuous methods for Volterra Integral Equations, Appl. Numer. Math. 119, 239-247 (2017).
[22] D. Conte, R. D'Ambrosio, M. Moccaldi, B. Paternoster, Adapted explicit two-step peer methods, J. Numer. Math., doi: 10.1515/jnma-2017-0102 (2018).

[23] D. Conte, R. D'Ambrosio, B. Paternoster, On the stability of ϑ-methods for stochastic Volterra integral equations, Discr. Cont. Dyn. Sys. - Series B 23(7), 2695–2708 (2018).
[24] D. Conte, R. D'Ambrosio, B. Paternoster, GPU acceleration of waveform relaxation methods for large differential systems, Numer. Algor., 71(2), 293–310 (2016).
[25] D. Conte, R. D'Ambrosio, Z. Jackiewicz, B. Paternoster, Numerical search for algebraically stable two-step continuous Runge-Kutta methods. J. Comput. Appl. Math. 239, 304-321 (2013).
[26] D. Conte, R. D'Ambrosio, B. Paternoster, Two-step diagonally-implicit collocation-based methods for Volterra Integral Equations, Appl. Numer. Math. 62 (2012), 1312-1324
[27] D. Conte, R. D'Ambrosio, Z. Jackiewicz, B. Paternoster, A practical approach for the derivation of algebraically stable two-step Runge-Kutta methods, Math. Model. Anal, 17 (1), 65-77 (2012),
[28] D. Conte, E. Esposito, L. Gr. Ixaru, B. Paternoster, Some new uses of the $\eta_m(Z)$ functions, Comput. Phys. Commun. 181, 128–137 (2010).
[29] D. Conte, Ixaru, L.Gr., Paternoster, B., Santomauro, G., Exponentially-fitted Gauss-Laguerre quadrature rule for integrals over an unbounded interval, J. Comput. Appl. Math. 255, 725–736 (2014).
[30] D. Conte, B. Paternoster, Modified Gauss-Laguerre Exponential Fitting Based Formulae, J. Sci. Comput. 69 (1), 227-243 (2016).
[31] D. Conte, Paternoster, B., G. Santomauro, An exponentially fitted quadrature rule over unbounded intervals, AIP Conf. Proc. 1479, 1173–1176 Springer (2012).
[32] D. Conte, B. Paternoster, Parallel methods for weakly singular Volterra Integral Equations on GPUs, Appl. Numer. Math. 114,30-37 (2017).
[33] D. Conte, B. Paternoster, A Family of Multistep Collocation Methods for Volterra Integral Equations, AIP Conf. Proc. 936, 128-131 (2007).
[34] R. D'Ambrosio, M. Moccaldi, B. Paternoster, F. Rossi, Adapted numerical modelling of the Belousov-Zhabotinsky reaction, J. Math. Chem. 56(10), 2867–2897 (2018).
[35] R. D'Ambrosio, M. Moccaldi, B. Paternoster, Parameter estimation in IMEX-trigonometrically fitted methods for the numerical solution of reaction-diffusion problems, Comp. Phys. Commun. 226, 55–66 (2018).
[36] R. D'Ambrosio, M. Moccaldi, B. Paternoster, Numerical preservation of long-term dynamics by stochastic two-step methods, Discr. Cont. Dyn. Sys. - Series B 23(7), 2763–2773 (2018).
[37] R. D'Ambrosio, M. Moccaldi, B. Paternoster, Adapted numerical methods for advection-reaction-diffusion problems generating periodic wavefronts, Comput. Math. Appl. 74(5), 1029–1042 (2017).
[38] R. D'Ambrosio, G. De Martino, B. Paternoster. General Nyström methods in Nordsieck form: error analysis, J. Comput. Appl. Math. 292, 694-702 (2016).
[39] R. D'Ambrosio, B. Paternoster, Numerical solution of reaction-diffusion systems of λ-ω type by trigonometrically fitted methods, J. Comput. Appl. Math. 294 C, 436-445 (2016).
[40] R. D'Ambrosio, B. Paternoster, A general framework for numerical methods solving second order differential problems. Math. Comput. Simul. 110(1), 113-124 (2015).
[41] R. D'Ambrosio, G. De Martino, B. Paternoster, Numerical integration of Hamiltonian problems by G-symplectic methods, Adv. Comput. Math. 40(2), 553-575 (2014).
[42] R. D'Ambrosio, G. De Martino, B. Paternoster, Order conditions of general Nyström methods, Numer. Algor., 65(3) 579-595 (2014).
[43] R. D'Ambrosio, E. Hairer, Long-term stability of multi-value methods for ordinary differential equations, J. Sci. Comput. 60(3), 627-640 (2014).
[44] R. D'Ambrosio, B. Paternoster, Numerical solution of a diffusion problem by exponentially fitted finite difference methods, SpringerPlus 3(1), 425-431 (2014).
[45] R. D'Ambrosio, B. Paternoster, Exponentially fitted singly diagonally implicit Runge-Kutta methods, J. Comput. Appl. Math. 263, 277-287 (2014).
[46] R. D'Ambrosio, B. Paternoster, G. Santomauro, Revised exponentially fitted Runge-Kutta-Nyström methods, Appl. Math. Lett. 30, 56-60 (2014).
[47] R. D'Ambrosio, E. Hairer, C. Zbinden, G-symplecticity implies conjugate-symplecticity of the underlying one-step method, BIT Numer. Math. 53, 867-872 (2013).
[48] R. D'Ambrosio, G. Izzo, Z. Jackiewicz, Search for highly stable two-step Runge-Kutta methods for ODEs, Appl. Numer. Math. 62(10), 1361-1379 (2012).
[49] R. D'Ambrosio, E. Esposito, B. Paternoster, Parameter estimation in exponentially fitted hybrid methods for second order ordinary differential problems, Journal of Mathematical Chemistry 50, 155-168 (2012).
[50] R. D'Ambrosio, E. Esposito, B. Paternoster, Exponentially fitted two-step Runge-Kutta methods: Construction and parameter selection, Appl. Math. Comp. 218 (14), 7468–7480 (2012).
[51] J.E. Ferrell, T.Y. Tsai, Q. Yang, Modeling the cell cycle: why do certain circuits oscillate?, Cell. 144(6), 874885 (2011).
[52] E. Francomano, M. Paliaga, Highlighting numerical insights of an efficient SPH Method, Appl. Math. Comput. 339, 899–915 (2018).
[53] E. Francomano, F. Hilker, M. Paliaga, E.Venturino, Separatrix reconstruction to identify tipping points in an eco-epidemiological model, Appl. Math. Comput. 318, 80–91 (2018).
[54] E. Francomano, M. Paliaga, Detecting tri-stability of 3D models with complex attractors via meshfree reconstruction of invariant manifolds of saddle points, Math. Meth. Appl. Sci. 41(17), (2018).
[55] E. Francomano, F. Hilker, M. Paliaga, E.Venturino An efficient method to reconstruct invariant manifolds of saddle points, Dolomites Research Notes in Approximation 10, 25–30 (2017).
[56] M.R. Garvie, J.F. Blowey, A reaction-diffusion system of λ-ω type. Part II: Numerical analysis, Euro. J. Appl. Math. 16, 621–646 (2005).
[57] J.M. Greenberg, Spiral waves for λ-ω systems, Adv. Appl. Math. 2, 450–455 (1981).
[58] E. Hairer, S. Norsett and G. Wanner, Solving ordinary differential equations I, Non-stiff problems, Springer, Berlin (1987)
[59] D. Hollevoet, M. Van Daele, G. Vanden Berghe, Exponentially-fitted methods applied to fourth order boundary value problems, J. Comput. Appl. Math. 235(18), 5380–5393 (2011).
[60] E. Isaacson, H.B.Keller, Analysis of Numerical Methods, Dover Publications, New York (1994).
[61] L. Gr. Ixaru, G. Vanden Berghe, Exponential Fitting, Kluwer, Boston-Dordrecht-London (2004).
[62] N. Kopell, L.N. Howard, Plane waves solutions to reaction-diffusion equations, Studies in Applied Mathematics 52, 291–328 (1973).
[63] B. Paternoster, Present state-of-the-art in exponential fitting. A contribution dedicated to Liviu Ixaru on his 70-th anniversary, Comput. Phys. Commun. 183, 2499–2512 (2012).
[64] W.E. Schiesser, The Numerical Method of Lines: Integration of Partial Differential Equations, Academic Press, San Diego (1991).
[65] W.E. Schiesser, G.W. Griffiths, A Compendium of Partial Differential Equation Models: Method of Lines Analysis with Matlab, Cambridge University Press (2009).
[66] J.A. Sherratt, Periodic waves in reaction-diffusion models of oscillatory biological systems, FORMA 11, 61-80 (1996).
[67] J.A. Sherratt, On the evolution of periodic plane waves in reaction-diffusion systems of λ-ω type, SIAM J. Appl. Math. 54, 1374–1385 (1994).
[68] J.A. Sherratt, M.J. Smith, Transition to spatiotemporal chaos via stationary branching shocks and holes, Physica D: Nonlinear Phenomena 241(15), 1671–1679 (2012).
[69] J.A. Sherratt, M.J. Smith, Periodic travelling waves in cyclic populations: field studies and reactiondiffusion models, J. Roy. Soc. Interface 5, 483–505 (2008).
[70] G.D. Smith, Numerical solution of partial differential equations - Finite difference methods, Clarendon Press, andOxford (1985).
[71] M.J. Smith, J.D.M. Rademacher, J.A. Sherratt, Absolute stability of wavetrains can explain spatiotemporal dynamics in reaction-diffusion systems of lambda-omega type, SIAM J. Appl. Dyn. Systems 8, 1136–1159 (2009).
[72] M.J. Smith, J.A. Sherratt, X. Lambin, The effects of density-dependent dispersal on the spatiotemporal dynamics of cyclic populations, J. Theor. Biol. 254(2), 264–274 (2008).
[73] M.J. Smith, J.A. Sherratt, The effects of unequal diffusion coefficients on periodic travelling waves in oscillatory reaction-diffusion systems, Physica D: Nonlinear Phenomena 236(2), 90–103 (2007).

Raffaele D'Ambrosio is Associate Professor at the Department of Engineering and Computer Science and Mathematics of University the of L'Aquila. He has been Fulbright Research Scholar in the Academic Year 2014-15 at Georgia Institute of Technology. His research interests cover numerical approximation of ordinary and partial differential equations, integral equations, Hamiltonian problems, stochastic differential equations, piecewise smooth dynamical systems, with particular emphasis to structure-preserving numerical integration.

Martina Moccaldi got her Ph.D. in Mathematics on December 2018. She is interested in the numerical discretization of partial differential equations and stochastic problems, with application to oscillatory chemical reactions.

Beatrice Paternoster is Full Professor of Numerical Analysis at University of Salerno, Italy. In her research she has focused her attention on the analysis and derivation of new and efficient numerical methods for functional equations, in particular differential and integral Equations. She is also interested in parallel computation, with concerns to the development of mathematical software for evolutionary problems.